




Review

Effects of Pore Size Parameters of Titanium Additively Manufactured Lattice Structures on the Osseointegration Process in Orthopedic Applications: A Comprehensive Review

Rashwan Alkentar ^{1,2,*} , Nikolaos Kladovasilakis ³ , Dimitrios Tzetzis ³  and Tamás Mankovits ²

¹ Doctoral School of Informatics, Faculty of Informatics, University of Debrecen, Kassai u. 26, H-4028 Debrecen, Hungary

² Department of Mechanical Engineering, Faculty of Engineering, University of Debrecen, Ótemető u. 2–4, H-4028 Debrecen, Hungary

³ Digital Manufacturing and Materials Characterization Laboratory, School of Science and Technology, International Hellenic University, 57001 Thessaloniki, Greece

* Correspondence: rashwan.alkentar@eng.unideb.hu

Abstract: Architected materials are increasingly applied in form of lattice structures to biomedical implant design for the purpose of optimizing the implant's biomechanical properties. Since the porous design of the lattice structures affects the resulting properties of the implant, its parameters are being investigated by numerous research articles. The design-related parameters of the unit cells for a strut-architected material are mainly the pore size and the strut thickness. Until today, researchers have not been able to decide on the perfect values of the unit cell parameters for the osseointegration process and tissue regeneration. Based on in vivo and in vitro experiments conducted in the field, researchers have suggested a range of values for the parameters of the lattice structures where osseointegration is in acceptable status. The present study presents a comprehensive review of the research carried out until today, experimenting and proposing the optimum unit cell parameters to generate the most suitable lattice structure for the osseointegration procedure presented in orthopedic applications. Additional recommendations, research gaps, and instructions to improve the selection process of the unit cell parameters are also discussed.

Keywords: architected materials; lattice structures; additive manufacturing; optimization; osseointegration



Citation: Alkentar, R.; Kladovasilakis, N.; Tzetzis, D.; Mankovits, T. Effects of Pore Size Parameters of Titanium Additively Manufactured Lattice Structures on the Osseointegration Process in Orthopedic Applications: A Comprehensive Review. *Crystals* **2023**, *13*, 113. <https://doi.org/10.3390/cryst13010113>

Academic Editor: Umberto Prisco

Received: 28 November 2022

Revised: 26 December 2022

Accepted: 5 January 2023

Published: 7 January 2023



Copyright: © 2023 by the authors. Licensee MDPI, Basel, Switzerland. This article is an open access article distributed under the terms and conditions of the Creative Commons Attribution (CC BY) license (<https://creativecommons.org/licenses/by/4.0/>).

1. Introduction

Bone replacement operations have increased the demand for the development of metallic biomaterials for implants [1]. Biomaterials gained recognition in the biomedical field after the meeting on biomaterials at Clemson University, South Carolina in 1969, due to their ability to improve the quality and longevity of the artificial parts inside the human body, especially of the implants used in human bone replacement surgeries [2]. The mechanical properties of the biomaterials should match those of the bone under loading during the activities of daily living (ADL). Bone's elastic modulus, for example, varies in range from 4 to 30 GPa according to the type of bone [3], hence, the material replacing the bone is expected to have a close value in that range. In case of stiffer implant material, the implant will absorb the whole stress, causing bone resorption around the implant area which leads to the loosening of the implant [4], commonly known as the stress-shielding effect.

The reaction of the human body to the implant decides the success or the failure of the biomaterial and tells how biocompatible it is [5]. Bioactive materials are preferable due to their integration with the surrounding bone [4]. Hallab et al. [6] emphasized that in order for the implants to have a long life span, their composing biomaterials should have high corrosion and wear resistance to avoid releasing non-compatible metal ions causing allergic

and toxic reactions in the implant area. Cobalt-based alloys, stainless steel, and titanium materials are widely used as biomaterials for implants [7] due to their superior mechanical properties and their high corrosion resistance [8]. Existing articles [9,10] have shown that exotic alloys, especially titanium alloys, revealed intense bioactivity properties along with enhanced bone fixation and durability. For these reasons and their great biocompatibility, as well as their lighter weight than other materials, titanium alloys have become the most widely used material in the manufacturing of implants [11]. Bich Vu et al. [12] evaluated the in vivo and the in vitro compatibility of the Ti6Al4V alloy and confirmed that it is suitable for use in medical implants. Furthermore, recent studies [13,14] have proposed the employment of ceramics and synthetic polymers as construction materials for orthopedic implants.

Hip implant surgeries and revision surgeries are increasing over the years, especially for people over 60 years old, for whom it was expected to double over the 2020–2050 range [15]. Worldwide, the annual number of hip injuries is expected to be over 6.26 million by 2050 [16]. A total of 15% of all the fractures in the United States were reported to be hip fractures, which means an extra 19 billion dollars to the national economy [17]. Slif et al. [18] performed a review on 225 patients who had 237 hip revision surgeries over a 6-year time period. The study reports 51.9% of the cause of failure to be aseptic loosening; 16.9%, instability; and 5.5%, infection. Therefore, many techniques have been experimented on to be added to the surface in order to improve the fixation ability of the implant when inside the human body [19].

Natural bones are porous materials in nature with interconnected pores, and they are classified based on their density as cancellous/trabecular bone and cortical bone. Cortical bone is strong and dense with a porosity of 5–10%, while the trabecular bone is more porous and weak with a porosity of 50–90% [20]. The hip implant usually causes some damage to the medullary space during the operation and results in a change in the endosteal circumference [21]. The blood supply in the endosteum causes resorption in the cortical bone, which might lead to a reduction in bone density. More medullary space for the hip implant proved better for medullary revascularization and improved blood circulation [21,22]. Yang et al. [23] proposed lightening the hip implant to get more surface space to provide proper medullary revascularization. If added to the implant surface, holes are proven to connect the inner and outer regions of the implant, thus providing better integration with the bone [24,25].

The most adopted method for getting the implant lightened and changing its surface into a porous area is the lattice structure configuration. Architected materials are three-dimensional structures composed of repeating unit cells that result in a completely porous body, known as lattice structures [26]. The edges and faces of the cells are usually formed by the struts and plates/surfaces [27]. The mechanical properties of lattice structures can be significantly affected by adjusting their defining parameters, such as unit cell topology or geometry (cell size/length and strut dimension) [28]. Mubasher Ali et al. [29] classified lattice structures into two main categories: beam-based and surface-based lattice structures.

Although beam-based lattice structures have simpler designs [30], they are chosen to help increase the efficiency of the material distribution inside the lattice pores [31]. When the concern is about manufacturability and bone fixation, surface-based lattice structures, especially triply periodic minimal surfaces (TPMS), offer extra advantages over beam-based ones. Yan et al. [32] stated that since the inclination of TPMS structures keeps changing along the 3D-printing process, this makes each layer support the next one in line, thus improving manufacturability. Designers suggest that the curvature in the surfaces of the implant directly affects the quality of bone ingrowth [33]. TPMS resembles the natural human trabecular bone, concerning geometrical topology and dimensional curvature. This resemblance improves the osseointegration more in comparison with the beam-based lattices [28].

The deformation of latticed structures is seen as an advantage for energy absorption-related applications [34], such as implant load bearing. Maskery et al. [35] investigated the

deformation behavior of Gyroids, a surface-based lattice type, and found that their specific energy absorption is three times better in comparison with the body-centered cubic lattices, a beam-based lattice type. Burton et al. [36] indicated that lattice structures have a void within their structure that can be filled with therapeutic agents without affecting the fatigue life of the load-bearing of the hip implant.

Additive manufacturing (AM) makes the manufacturing of complex lattice structures possible due to the layer-by-layer building mechanism [37]. Yan et al. [38] studied the microstructure and mechanical properties of the lattice structures manufactured via direct metal laser sintering (DMLS), an AM technology, and stated that the latter outperforms lattice structures made by alternative manufacturing techniques with the same porosity. Each AM technique has certain abilities and constraints in the manufacturing of lattice structures. Cansizoglu et al. [39] investigated the properties of Ti6Al4V lattice structures manufactured via electron beam machining (EBM), another AM method, using compression, bending tests, and finite element analysis. The study reported that build angle and build orientation strongly affected the properties of the lattice structures.

The current study aims to deeply review the latest literature and discuss the research gaps on the effect of the pore design of the lattice structure on the bone ingrowth process. In detail, Section 2 focuses on the narrative review of the bone structures, up-to-date use of implants, and the biofunctionality mechanisms that activate during implant placement. Furthermore, Section 3 presents the existing architected materials (definition and classification) coupled with the impact of porosity/relative density on the mechanical properties of a lattice structure, according to the published literature. In addition, Section 4 summarizes, in a comprehensive review, the results of numerous studies regarding the effect of pore/porosity of structure in osseointegration processes. Finally, in Section 5, the main research gaps and current challenges are highlighted along with proposals for future investigation in the field.

2. Implants, Bone Structure, and Biofunctionality Mechanisms

2.1. Implant Structures and Materials

Since the ancient era, orthopedic implants have been utilized in order to assist and facilitate bone tissue recovery from injuries [40]. Through the years, the implementation of implants has evolved in terms of materials, biofunctionality, and structure. In the last century, the evolution of surgery methods coupled with the development of sophisticated imaging techniques, such as the computed tomography scan (CT scan), magnetic resonance imaging (MRI), etc., led to great improvements in medical implants generally [41]. Despite the evolution of implants, some basic principles should be followed in implant development, such as high biocompatibility and the facilitation of tissue regeneration. In this context, the human implants are classified into three generations based on their chronological evolution according to the existing literature [42–44], as is shown in Figure 1. The first generation, the oldest one, includes implants developed only for the purposes of the fixation and support of the damaged tissue, and they were bioinert without any interaction with the surrounding biological system [45]. In the second generation, the implants' materials and structure not only offer the proper structural integrity but also facilitate the diffusion of blood and nutrients, achieving higher biocompatibility [46]. In this category, the orthopedic hip implants of Trilock type are included with their unique characteristic of lattice regions inside their structure. The third and more recent generation of implants consists of implants with the above-mentioned characteristics along with biomimetic and bioactive structures [43,47]. Furthermore, the implants of the third generation could be enhanced with the existence of growth factors on their external surface, in the form of coatings, to accelerate the tissue regeneration process. In addition, it could be constructed with biodegradable and bioabsorbable materials in order to be absorbed by the human body and avoid surgery for implant removal [8,13]. These comprehensive reviews [8,13] analyzed the advantages of the third generation implants to be the biodegradable and

bioabsorbable construction materials, the hydroxyapatite (HA) coatings of implants, as a growth factor, and the implementation of biomimetic geometry.

Before the investigation of the effect of structure (porosity) on an implant's performance, it is essential to present the available biomaterials for this application, the bone structure, and the major phenomena that have been developed on an orthopedic implant in order to better understand the operating condition. First of all, the term "biomaterials" refers to materials that interact with biological systems (organs, tissue, etc.), facilitating the tissue regeneration procedure without any unfavorable consequences, i.e., carcinogenesis, thrombogenesis, toxicity, irritation, and immunogenesis [14,48]. For orthopedic applications, metals and metal alloys (titanium, titanium alloys, stainless steel, Co-Cr alloys) are mainly utilized considering their superior mechanical properties and their high corrosion resistance [49]; however, some recent studies [48,50] have proposed the employment of ceramics and synthetic polymers as construction materials. On the other hand, the structure of a human bone has high geometric complexity, and it is crucial to analyze it thoroughly in order to improve the implant's functionality. A typical human bone consists of three regions: the cortical, the osteon, and the cancellous bones [51,52]. The cortical region is bulk bone tissue located in the external layers of the bone with high stiffness, more specifically with an elastic modulus ranging from 14 to 20 GPa [53], offering structural integrity to the bone's structure. Moreover, cortical bones reach up to 80% of the overall bone mass. The osteon is located in the region between the cortical and cancellous bone and provides the necessary diffusion canals, such as the Haversian and Volkmann's canals, for the circulation of blood and nutrients. Finally, the cancellous bone has the highest volume in a bone structure; however, it roughly reaches 20% of overall bone mass due to its extensive porosity that ranges from 50% to 90%. The porosity consists of stochastic strut lattices with highly variable porosity, lower near the osteon and cortical bone and higher in the center of the bone [53]. Furthermore, the cancellous bones provide elasticity, with its elastic modulus ranges between 3.2 and 12.7 GPa [54] depending on the regional porosity, and energy absorption capabilities on the bone with sufficient volume from bio-reactions, such as blood cell production, etc. Figure 2 portrays a detailed illustration of an indicative bone structure [52]. Hence, in the last decade, the integration of pore structures, such as lattice structures, with architected materials in implant design has gained increased scientific interest in an attempt to bio-mimic the bone structure and enhance its biocompatibility.

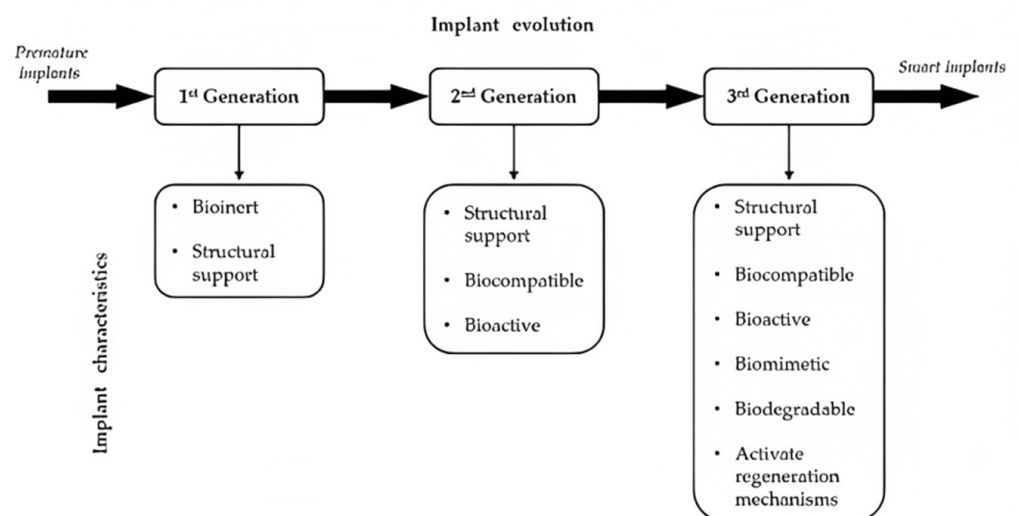


Figure 1. Description of implant evolution divided into three generations coupled with their main characteristics [52].

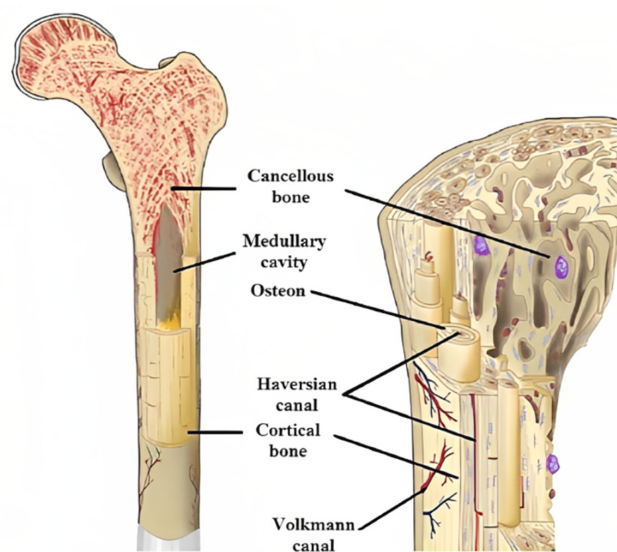


Figure 2. Indicative image of a human bone structure [52].

2.2. Biocompatibility and Failure Mechanisms for an Implant

In the previous subsection, the classification of medical implants based on their evolution was discussed coupled with the methods, i.e., biomaterials and advanced structures, to produce a bone implant with high biocompatibility. Moreover, in order to develop the optimum pore structure for an implant, it is necessary to understand the major phenomena occurring in the biological systems with foreign objects such as implants, namely wear, stress-shielding, and osseointegration [55–57]. In detail, osseointegration is responsible for the tissue regeneration process and efficiency of the implant, and the other two phenomena are mainly responsible for the failure of an implant. It is worth mentioning that these phenomena have a different magnitude in each case depending on several reasons besides the implant (type of injury, surgical procedure, etc.) [48]. However, the porous structure of an implant has a severe impact on the regulation of these mechanisms.

Wear is a mechanism of failure for an implant and occurs on the interface between the bone and the implant [56]. More specifically, during the activity of daily living (ADL), relative movements between the implant and the bone are observed to lead to the development of friction forces on the interface surfaces, resulting in material removal and bone deformation. Existing studies [56,58] have shown that wear is responsible for the osteolytic reaction, loosening, and reduction of the implant's life. All these eventually result in the implant's failure. In order to address this issue, the increase of the friction coefficient between the bone and the implant has been proposed by minimizing their relative movement. There are two sufficient methods to increase the friction coefficient between the bone and the implant. The first is the increase of the roughness of implant surfaces during the manufacturing process, and the second is the employment of superficial pore structures around the implant, as the lattice structures have revealed an increased friction coefficient [58]. A commercial example of this method is the Trilock hip implant, which has demonstrated remarkable durability.

The stress-shielding effect occurs mainly in metal implant applications due to the superior mechanical properties of metal alloys [59,60]. Human bones are highly adaptive at loading conditions, increasing their mass in regions with high-stress concentration and vice versa. Hence, the bone starts to lose its mass and its structural integrity due to the difference in stiffness between the metal implant and the bone. More specifically, when a metal implant is employed in the human body, the majority of loads are absorbed by the metal structure, leading to a low-stress concentration on the bone regions. Combining the aforementioned observations, the bone can reveal osteopenia or osteoporosis and, in some cases, even bone fracture. Thus, it is essential to minimize this phenomenon by reducing the

difference in stiffness between the bone and the metal implant. The reduction of implants' stiffness can be achieved in two ways. The first is the replacement of the construction metal with a material with a lower elastic modulus (i.e., stiffness); however, for bone applications, it is difficult to find a material with enhanced strength and low stiffness. Therefore, in order to address this phenomenon, the majority of the literature examined the employment of pore structures/lattice structures within the body of the implant. Lattice structures consist of architected materials enabling topology-controlled properties [59]. In detail, according to existing research [61], lattices reveal a lower stiffness than bulk structures for the same construction material due to the porosity of the structure. Moreover, the reduction in stiffness could be accurately calculated via the scaling law on the mechanical properties of the structure, as analyzed in the next section.

Osseointegration is the desired phenomenon for an implant and describes the structural and functional connection between the bone and the implant [62–64]. In order to facilitate the osseointegration effect, the implant should provide the necessary space to diffuse blood/nutrients and a sufficient surface area for the cell to adhere to and enable cell production and regeneration via osteoconductivity. Especially in bone implants, the bone healing process requires several weeks and enough space, first, for the diffusion of soft callus cartilage and fibrous tissues which form the premature bone, and then, for the regeneration of hard bone, also known as hard callus tissue [65]. It is obvious that in order to be able to achieve a proper bone regeneration procedure, it is essential to employ the porous structures and surface porosity in the implants. In addition, porous structures offer a high surface area-to-volume ratio providing extensive surface area for cell adhesion and bioreactions.

By revising the major phenomena that occur on the bone implant inside the human body, it is logical to derive the conclusion that the architected materials in the form of lattice structures provide the necessary properties in order to address them. However, each architected material has its own unique physical (i.e., pore shape, surface area to volume ratio, etc.) and mechanical properties (i.e., effective mechanical properties), thus, in the context of this review, it is essential to analyze the influence of the geometry/pores of architected materials on the biofunctionality and biocompatibility of an implant.

3. Architected Materials on Biomechanical Applications

3.1. Definition and Classification of Architected Materials

As it was mentioned in the previous section, the implementation of architected materials, in form of lattice structures, on bone implants offers a series of advantages for the biofunctionality of the implant. Therefore, there is a need to analyze and classify the existing architected materials. Architected materials are multiphase and/or cellular materials in which the topological distribution of the phases is carefully controlled and optimized for specific functions or properties [66]. Their basic physical properties are the relative density ($\bar{\rho}$) or porosity (p) of the structure, which are derived from the volume of solid material (V_{Solid}) to the overall external volume of the structure (V_{BB}), i.e., bounding box. Equations (1) and (2) show how to calculate the relative density and the porosity of an architected material, respectively.

$$\bar{\rho} = \frac{V_{\text{Solid}}}{V_{\text{BB}}} \quad (1)$$

$$p = 1 - \bar{\rho} = 1 - \frac{V_{\text{Solid}}}{V_{\text{BB}}} \quad (2)$$

Depending on the applied relative density of an architected material, three categories are derived. The foam-like structures with an ultra-low relative density below 5%, the lattice structures with a relative density from 20% to 50%, which are the most commonly used architected materials, and the structures with a relative density above 60%, which have a mechanical response very close to the bulk material [67]. According to the existing literature [68,69], the relative density of every architected material depends on the ratio of

two design-related parameters, namely the strut/wall thickness (t) to the length of the unit cell (l). In detail, based on the nature of the employed architected material, approximate mathematical formulations have been developed connecting the relative density with the t/l ratio. Equations (3) and (4) present the abovementioned formulation for two of the most widespread lattice structures, the struts and the triply periodic minimal surfaces (TPMS). It is worth noting that C_1 , C_2 , and C_3 are constants, different for each architected material, and are derived from the topology of each structure.

$$\text{Strut-lattice structures : } \bar{\rho} = C_1 \cdot \left(\frac{t}{l}\right)^2 - C_2 \cdot \left(\frac{t}{l}\right)^3 \quad (3)$$

$$\text{TPMS lattice structures : } \bar{\rho} = C_3 \cdot \left(\frac{t}{l}\right) \quad (4)$$

After the definition and the analysis of the most crucial parameters for architected materials, the next step is to classify them based on their geometry, as there is a vast number of different geometries [70,71]. It is worth mentioning that in the context of this review, the architected materials with open cells were taken into account due to the creation of diffusion canals inside the structure, which are essential for biomechanical applications. The first level of classification concerns the periodicity of the architected material and divides them into three categories: stochastic, periodic, and pseudo-periodic [70,71]. Open-cell stochastic architected materials are usually observed in natural structures, such as cancellous bone, corals, etc. However, they can be artificially developed by employing stochastic algorithms and geometric loci, such as Voronoi. The examination and regulation of the properties of these structures are quite difficult processes due to the stochastic nature of the structures. On the other hand, there are periodic architected materials, also known as cellular materials, with open cells that consist of a single 3D unit cell that is repeated in the three dimensions. It is necessary to mention that the 2.5D architected materials (i.e., honeycombs, prismatic, etc.) were not taken into account in this classification due to the lack of interconnected canals/pores. Three-dimensional architected materials of strut and TPMS are the most commonly used lattice structures with interconnected pores, i.e., open cells. Finally, there are the pseudo-periodic structures that are consisted of the above-mentioned architected materials with the major characteristic of interaction of the structure's boundaries with the lattice structure. Figure 3 presents a detailed diagram with geometry-based classification for open-cell architected materials [71,72].

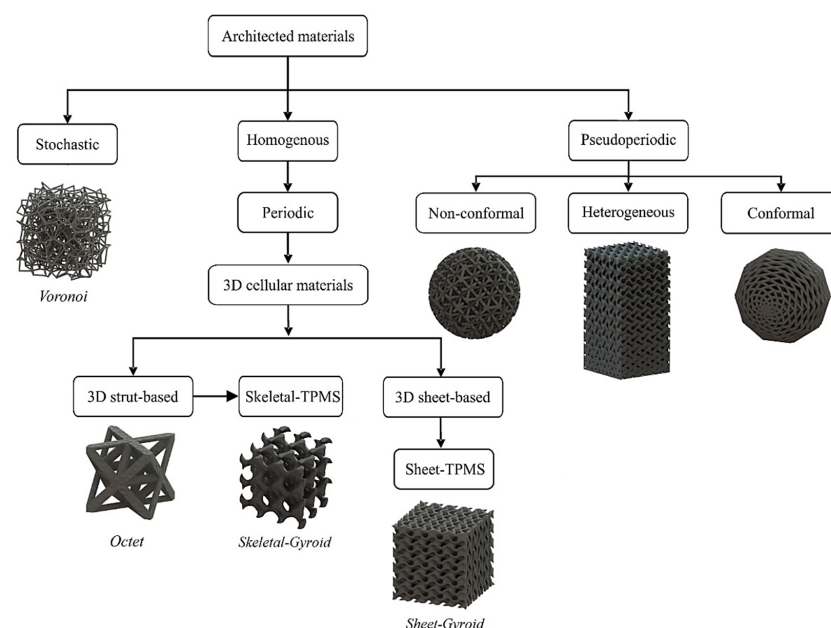


Figure 3. Classification diagram of architected materials with open cells based on the geometry [71,72].

3.2. Influence of Pores on Architected Materials Properties

Having discussed the basic characteristics and classification of architected materials, it is essential to analyze the influence of pore size/porosity on the physical and mechanical behavior of a lattice structure. It is obvious that as the porosity increases in a lattice structure, more void space inside the structure is created, facilitating the potential diffusion of material. Thus, it is usually proposed that the porosity percentage of a lattice structure embedded in a metal implant should have a similar value to the porosity of the cancellous bone, leading to a mean relative density of around 20%. However, this can raise some issues concerning the implant's biofunctionality and biocompatibility. The first issue is related to the degradation of the mechanical properties of the structure due to the increased porosity. According to existing studies [67,73,74], the degradation of the mechanical properties (Φ) of a lattice structure follows a scaling/power law strongly influenced by the applied relative density/porosity. Equation (5) lists the aforementioned scaling law applicable to the majority of the mechanical properties (elastic modulus, yield strength, etc.).

$$\Phi = C \cdot (\bar{\rho})^n \quad (5)$$

where C and n are constants that are dependent on the applied construction material and the applied architected material. Therefore, the applied architected material defines the rate of degradation of the properties as the relative density decreases. If the employed cellular material has low connectivity ($n > 2$), the rate of degradation is exponential and is observed in the bending deformation of the structure's elements, hence this mechanical response is named bending-dominated behavior [75,76]. Lattice structures with bending-dominated behavior have relatively low strength and stiffness with enhanced energy absorption rates. On the other hand, the architected materials with linear degradation ($n \approx 1$) of properties in changes of relative density show high connectivity and reveal high stiffness and strength [75,76]. This mechanical response is the stretching-dominated behavior, and this kind of architected material is usually utilized for bone implant applications due to the high strength requirements. In addition, published research [77] has proved the connection between the relative density and the available surface area in a lattice structure for certain architected materials. The available surface area seems to decrease in very low and very high relative densities. Moreover, TPMS lattice structures, especially sheet-TPMS, reveal a higher surface area-to-volume ratio compared with the strut lattices, making them suitable for biomechanical applications [77].

Throughout the process of adjusting the porosity of the lattice structure to fit the biointegration process, Jayanthi [78] pointed out that the effective compressive strength of the titanium structure drops with the increasing porosity. Figure 4, along with Table 1, shows the relationship between porosity and compressive strength for porous titanium which helps with trading off between the porosity and the required strength.

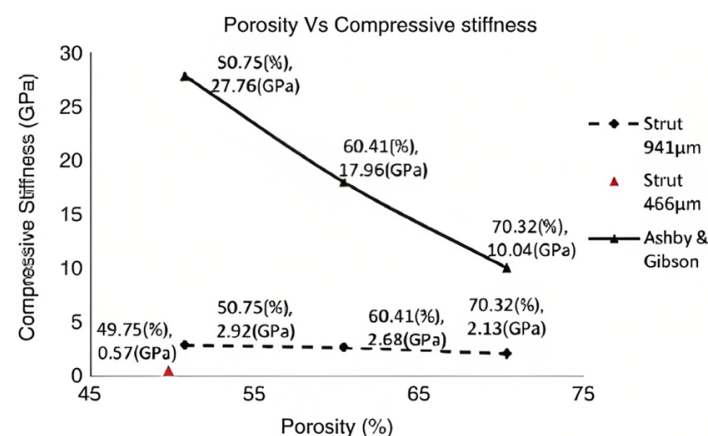


Figure 4. Porosity vs. compressive stiffness. Reused with permission from ref. [78]. 2009, Elsevier Ltd.

Table 1. Compressive stiffness and compressive strength of porous titanium parts. Reprinted with permission from ref. [78]. 2009, Elsevier Ltd.

Set	Porosity	Comp. Stiffness (GPa)	Ultimate Comp. Strength (MPa) σ_{max}	Maximum Load (N)
1	50.75 (10.69)	2.92 (± 0.17)	163.02 (111.98)	36,759
2	60.41 (± 0.81)	2.68 (± 0.12)	117.05 (1554)	25,224
3	70.32 (± 0.63)	2.13 (± 0.21)	83.13 (± 10.25)	18,985
4	49.75 (± 1.00)	0.57 (± 0.05)	7.28 (10.93)	1506

To summarize, the properties of an implant with lattice structures are influenced by the relative density/porosity of the applied architected material. Porosity has a severe impact on the mechanical performance of the implant. Thus, it is essential for each architected material embedded in an implant to find the optimum value of porosity/pores in order to withstand the applied loads while simultaneously minimizing the stress-shielding effect. Moreover, the porosity of the applied structure should be defined at the proper value in order to be capable of diffusing the blood and nutrients, but also provide sufficient surface area to adhere cells for osseointegration and tissue regeneration. For these reasons, the next section presents a comprehensive review of up-to-date research on the effect of pores on the biofunctionality and biocompatibility of a bone implant.

4. Effect of Pore Size Parameters on the Osseointegration Process

The process of bone ingrowth into an implanted structure is extremely complicated and involves a wide range of factors, including cellular and extracellular biological activities [79]. The fixation stability of the implant is also an important factor in the success of the osseointegration process [80]. The architecture of the implanted biomaterial with lattice structures has a significant role in the osseointegration process, which leads to the conclusion that the unit cell topology, porosity, pore size and shape have a strong effect on bone ingrowth [81–83]. Arabnejad et al. [84] investigated four samples of two unit-cell types, Tetrahedron and Octet truss, with parameters from a limited area of selection suitable for bone ingrowth and set according to previous experiments [85–87]. The selection area for the Tetrahedron topology was defined by the following parameters: the pore size was between 50–800 μm , the porosity was at least 50%, and the strut thickness lowest limit was set to 200 μm , due to manufacturing constraints where most of the commonly used AM techniques can build lattice materials with a nominal strut thickness of 200 μm [88]. The design limit values for the Tetrahedron type are shown as red lines in Figure 5. It is worth mentioning that there are AM techniques which are able to fabricate structures at the nanometer level, such as the two-photon polymerization (2PP) technology; however, these technologies have specific miniaturized applications and are not applicable for biomechanical applications on centimeter levels.

For the Octet truss type, the design limits were a 400–800 μm pore size, 50% porosity and strut thickness of 200–400 μm . The design area of the Octet truss type is shown in Figure 6.

The samples were then implanted in two mongrel dogs for bone ingrowth monitoring purposes. The study confirmed the immediate relationship between the parameters of the unit cells and their strong effect on the osseointegration process [84]. Bragdon et al. [85] performed eight total hip replacements on eight animals and monitored the improvement over a three-month period. The study found that pore size and porosity had an obvious effect on the osseointegration process and stated that latticed implants with a mean pore size $\geq 200 \mu\text{m}$ and a porosity $\geq 40\%$ were optimal for bone ingrowth, yet the study did not set an upper limit for the pore size or for the porosity. Through an in vivo study, Whang et al. [89] set the minimum pore size to allow bone ingrowth to be 100–350 μm , but did not study the ranges of porosity or thickness of the structures.

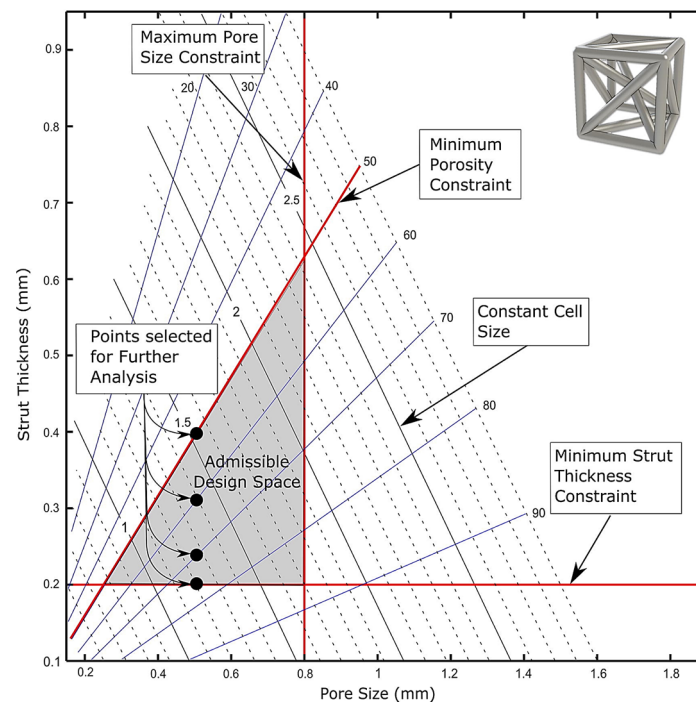


Figure 5. Design area for Tetrahedron topology, with the constraints of manufacturing, pore size, and porosity. Reprinted with permission from ref. [84]. 2016, Elsevier Ltd.

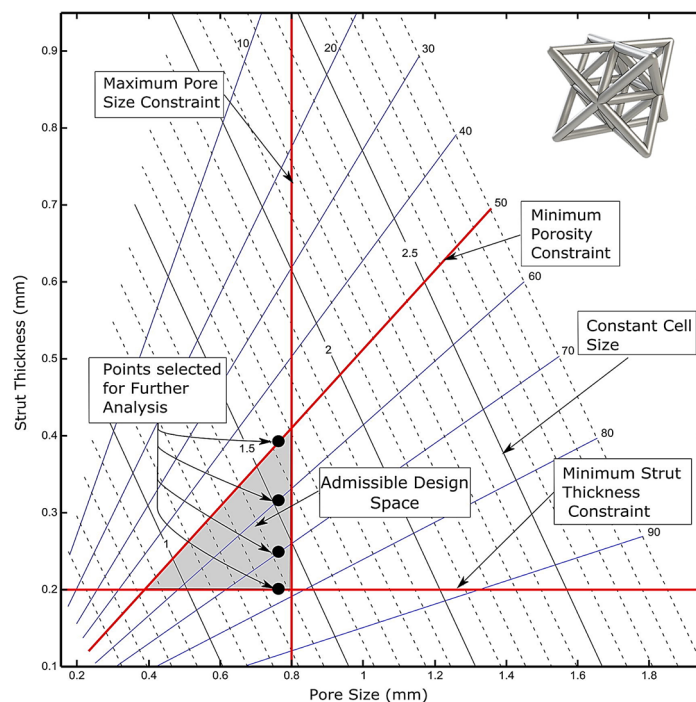


Figure 6. Design area for Octet truss with the constraints of manufacturing, pore size, and porosity. Reprinted with permission from ref. [84]. 2016, Elsevier Ltd.

In vitro studies showed that pore size had no direct effect on the formation of bones, but that a lower porosity enhanced bone regeneration. On the contrary, in vivo studies stated that in an atmosphere where osteogenesis dependent on many processes, such as vascularization, a higher porosity supported bone ingrowth the best. Pore sizes over 30 μm are better for the enhanced formation of bone and capillaries [87]. Taniguchi et al. [90] performed an in vivo study on rabbits where porous titanium implants with pore sizes of

300, 600, and 900 μm were manufactured by the selective laser melting (SLM) AM technique. The 600 μm pore-sized implants showed higher fixation and better osseointegration than the rest of the implants. Bone ingrowth within the 300 μm pore-sized implants was inferior in cancellous bone in comparison to the other-sized implants. Bone ingrowth into implants with a porosity of 50% and a pore size of 100–300 μm was able to reduce the stress-shielding effect dramatically [91]. For orthopedic applications, most implants have an average range of 400–600 μm for the pore size and 75–85% for the porosity [92]. A group of lattice structures averaging 430 μm and another group averaging 650 μm were investigated. The new bone was occupying 42% of the pores in the 4th week, 63% in the 16th week, and 80% at the end of the year. The bone ingrowth in the large-averaging group was 13% in the 2nd week, 53% in the 4th week, and 70% by the 52nd week.

Wang et al. [93] tested a trabecular-like lattice structure with 3 different pore sizes of 800, 900, and 1000 μm . In this study, the Ti6Al4V alloy was employed as a construction material. Elastic modulus was reduced with this type of structure, which helped avoid stress concentration and enhance proliferation, which, in turn, supports the osseointegration process. The irregular structure suggested in the study proved to have good mechanical properties. Research exhibited that the optimum porosity should be over 50% for good osseointegration, and pore size should be between 100–700 μm to avoid pore occlusion and to provide enough surface area for cell adhesion [84,94]. Haizum et al. [95] investigated Gyroid (surface-based lattice) and cube lattice structures (beam-based lattice) manufactured using SLM of Ti6Al4V alloy with 300–600 μm pore sizes. The study confirmed that a pore size of 300 μm generated structures similar to the natural bone and they can be used for orthopedic applications.

Triply periodic minimal surfaces (TPMS), a surface-based unit cell type, with a porosity range of 80–90% and a pore size range of 560–1600 μm were investigated for bone implants. They exhibited a very close structure compared to the trabecular bone in terms of all biomechanical properties [96]. During a general study, in vivo and in vitro, porous Ti6Al4V samples of cylinder porous structures with pore sizes 500, 700, and 900 μm were manufactured using the SLM system. Compression tests, CT scans, and scanning electron microscope (SEM) scans were performed to analyze and compare with the mechanical properties of the natural bone. The in vivo study showed that implants with a pore size of 600 μm helped enhance bone ingrowth maturation and fixation in the host body [97]. When the pore size of the lattice structure is below 200 μm , it becomes hard for the blood vessels to grow into the pores, which causes a lack of oxygen and nutrients. This, in turn, reduces the formation of new bone [98]. Table 2 shows a brief summary of all the values of the unit-cell parameters suggested by the above-mentioned studies.

Table 2. A summary of the unit-cell parameters.

Study	Suggested Pore Size [mm]	Suggested Strut Thickness [mm]	Porosity %
Arabnejad et al. [84]	0.2–0.8	≥ 0.2	≥ 50
Bragdon et al. [85]	≥ 0.2	-	≥ 40
Whang et al. [89]	0.1–0.35	-	-
Wang et al. [93]	0.1–0.7	-	≥ 50
Haizum et al. [95]	0.3–0.6	-	-
Yan et al. [96]	0.56–1.6	-	80–90
Qichun et al. [97]	0.6	-	-
Zheng et al. [98]	≥ 0.2	-	-

5. Research Gaps and Current Challenges

Although lattice structure is widely accepted as a solution to support the osseointegration process, its pore size is still under investigation. As seen in the above-mentioned literature, the ranges for an optimum pore size differ among researchers. A wide range of 50–1200 μm pore size was suggested by many reports; however, the optimum pore size for

implants still has not been defined [99]. Most AM techniques have manufacturing limits that affect the pore size's lowest value. SLM and EBM, for example, are able to produce a nominal strut thickness of 200 μm [84]. This limit is dependent on the process [86,88], and can be lower in different cases [100,101].

Although a high porosity percentage of 50–80% is preferable for better osseointegration, it affects the mechanical properties such as the strength and the stiffness of the structure [78,102]. As it was mentioned in Section 3, the type of the employed architected material plays a significant role in the mechanical performance. Besides the fact that many recent studies have examined the mechanical behavior of various architected materials, there is a lot of ground that should be covered due to the vast number of existing structures and the development of new ones with superior properties, such as the hybrid cellular materials [103,104].

Furthermore, one more aspect that has not been investigated thoroughly yet is the extracted structure's porosity in AM of the lattice structure. In detail, as it is commonly known, all AM techniques fabricate objects with a certain porosity. For example, in the SLM technique with proper optimization on process-related parameters, this porosity could be reduced to below 0.5% for bulk specimens [105]. However, studies [106,107] have shown that during the fabrication of lattice structures, this process-related porosity could be increased. Thus, it is essential to calculate the extracted porosity based on the implemented structure (strut-based or surface-based) and evaluate its impact on the osseointegration processes. Finally, further examinations should be performed on pore structures coated by growth factors in clinical trials to quantify the influence of both pore structure and growth factors on the biocompatibility and osseointegration of an implant.

Another less-examined area on the implementation of pore structures on implants is the role of the post-processing procedure on the outcome. Post-processing could reduce the roughness and enhance the dimensional accuracy of the implant; therefore, their influence on the biocompatibility of an implant is an area that should be examined further in the future.

6. Conclusions

This study reviews the effect of the pore size of the titanium lattice structures manufactured using AM on the osseointegration process. AM techniques help build all complex types of unit cells with the option of adjusting the building parameters as required. Changing the parameters of the unit cells, i.e., strut thickness and pore size, can significantly affect the mechanical properties of the whole structure. By manipulating these parameters, designers can generate lattice structures that suit the bone to be replaced.

Most researchers try to investigate the best combination between pore size and strut thickness to generate an implant with the lattice structure's porosity, that allows for bone ingrowth to an acceptable level, hence boosting osseointegration. Based on the literature discussed above, it is possible to say that, for optimum osseointegration in orthopedic applications, the best ranges for pore size, strut thickness, and porosity are 500–750 μm , 200–500 μm , and 50–90%, respectively. It is worth mentioning that the strut thickness lowest value was affected by the manufacturing limit in most of the AM techniques where the accuracy of manufacturing is at that level.

Yet, no definitive answer for the exact pore size is set. Since each type of bone in the human body has different mechanical properties, each type of unit cell is being investigated to have a pore size that results in a structure that matches a specific bone. Gaining some desired properties seems difficult to achieve without trading some others. Increasing porosity is hard without decreasing the mechanical strength, a fact that makes investigating the best pore size more and more necessary.

Author Contributions: Conceptualization, R.A. and N.K.; methodology, N.K.; validation, T.M. and D.T.; formal analysis, N.K.; investigation, D.T.; resources, R.A.; writing—original draft preparation, R.A., and N.K.; writing—review and editing, R.A.; visualization, N.K.; supervision, D.T. and T.M.; project administration, T.M. All authors have read and agreed to the published version of the manuscript.

Funding: This research received no external funding.

Conflicts of Interest: The authors declare no conflict of interest.

References

1. Park, J.B.; Lakes, R.S. (Eds.) *Metallic Implant Materials BT—Biomaterials*; Springer: New York, NY, USA, 2007; pp. 99–137. [\[CrossRef\]](#)
2. Ramakrishna, S.; Mayer, J.; Wintermantel, E.; Leong, K.W. Biomedical Applications of Polymer-Composite Materials: A Review. *Compos. Sci. Technol.* **2001**, *61*, 1189–1224. [\[CrossRef\]](#)
3. Katz, J.L. Anisotropy of Young's Modulus of Bone. *Nature* **1980**, *283*, 106–107. [\[CrossRef\]](#)
4. Geetha, M.; Singh, A.K.; Asokamani, R.; Gogia, A.K. Ti Based Biomaterials, the Ultimate Choice for Orthopaedic Implants—A Review. *Prog. Mater. Sci.* **2009**, *54*, 397–425. [\[CrossRef\]](#)
5. Williams, D.F. On the Mechanisms of Biocompatibility. *Biomaterials* **2008**, *29*, 2941–2953. [\[CrossRef\]](#) [\[PubMed\]](#)
6. Hallab, N.J.; Anderson, S.; Stafford, T.; Glant, T.; Jacobs, J.J. Lymphocyte Responses in Patients with Total Hip Arthroplasty. *J. Orthop. Res.* **2005**, *23*, 384–391. [\[CrossRef\]](#) [\[PubMed\]](#)
7. Okazaki, Y.; Gotoh, E. Comparison of Metal Release from Various Metallic Biomaterials In Vitro. *Biomaterials* **2005**, *26*, 11–21. [\[CrossRef\]](#)
8. Arcos, D.; Vallet-Regí, M. Substituted Hydroxyapatite Coatings of Bone Implants. *J. Mater. Chem. B* **2020**, *8*, 1781–1800. [\[CrossRef\]](#)
9. Ibrahim, M.Z.; Sarhan, A.A.D.; Yusuf, F.; Hamdi, M. Biomedical Materials and Techniques to Improve the Tribological, Mechanical and Biomedical Properties of Orthopedic Implants—A Review Article. *J. Alloys Compd.* **2017**, *714*, 636–667. [\[CrossRef\]](#)
10. Regis, M.; Marin, E.; Fedrizzi, L.; Pressacco, M. Additive Manufacturing of Trabecular Titanium Orthopedic Implants. *MRS Bull.* **2015**, *40*, 137–144. [\[CrossRef\]](#)
11. Davis, J.R. *Handbook of Materials for Medical Devices*; ASM: Novelt, OH, USA, 2003.
12. Vu, N.B.; Truong, N.H.; Dang, L.T.; Phi, L.T.; Ho, N.T.-T.; Pham, T.N.; Phan, T.P.; Van Pham, P. In Vitro and In Vivo Biocompatibility of Ti-6Al-4V Titanium Alloy and UHMWPE Polymer for Total Hip Replacement. *Biomed. Res. Ther.* **2016**, *3*, 14. [\[CrossRef\]](#)
13. González-Henríquez, C.M.; Sarabia-Vallejos, M.A.; Rodríguez-Hernández, J. Polymers for Additive Manufacturing and 4D-Printing: Materials, Methodologies, and Biomedical Applications. *Prog. Polym. Sci.* **2019**, *94*, 57–116. [\[CrossRef\]](#)
14. Bazaka, O.; Bazaka, K.; Kingshott, P.; Crawford, R.J.; Ivanova, E.P. Chapter 1 Metallic Implants for Biomedical Applications. In *The Chemistry of Inorganic Biomaterials*; The Royal Society of Chemistry: London, UK, 2021; pp. 1–98. [\[CrossRef\]](#)
15. Agency for Healthcare Research and Quality. *Exhibit 19. HCUP Estimates of the Total Number of Target Procedures*; Agency for Healthcare Research and Quality: Rockville, MD, USA, 2012.
16. Cooper, C.; Campion, G.; Melton, L.J., 3rd. Hip Fractures in the Elderly: A World-Wide Projection. *Osteoporos. Int.* **1992**, *2*, 285–289. [\[CrossRef\]](#) [\[PubMed\]](#)
17. Kamel, H.K. Postmenopausal Osteoporosis: Etiology, Current Diagnostic Strategies, and Nonprescription Interventions. *J. Manag. Care Pharm.* **2006**, *12* (Suppl. S6), S4–S9, S26–S28. [\[CrossRef\]](#) [\[PubMed\]](#)
18. Ulrich, S.D.; Seyler, T.M.; Bennett, D.; Delanois, R.E.; Saleh, K.J.; Thongtrangan, I.; Kuskowski, M.; Cheng, E.Y.; Sharkey, P.F.; Parvizi, J.; et al. Total Hip Arthroplasties: What Are the Reasons for Revision? *Int. Orthop.* **2008**, *32*, 597–604. [\[CrossRef\]](#)
19. Pilliar, R.M. Powder Metal-Made Orthopedic Implants with Porous Surface for Fixation by Tissue Ingrowth. *Clin. Orthop. Relat. Res.* **1983**, *176*, 42–51. [\[CrossRef\]](#)
20. Sikavitsas, V.I.; Temenoff, J.S.; Mikos, A.G. Biomaterials and Bone Mechanotransduction. *Biomaterials* **2001**, *22*, 2581–2593. [\[CrossRef\]](#) [\[PubMed\]](#)
21. Pazzaglia, U.E.; Zatti, G.; Cattaneo, S.; Cherubino, P. Evaluation of Hollow and Full Stems Implanted in the Rabbit Tibia: Preliminary Results. *Biomaterials* **1993**, *14*, 883–886. [\[CrossRef\]](#)
22. Pazzaglia, U.E. Periosteal and Endosteal Reaction to Reaming and Nailing: The Possible Role of Revascularization on the Endosteal Anchorage of Cementless Stems. *Biomaterials* **1996**, *17*, 1009–1014. [\[CrossRef\]](#)
23. Yang, C.-T.; Wei, H.-W.; Kao, H.-C.; Cheng, C.-K. Design and Test of Hip Stem for Medullary Revascularization. *Med. Eng. Phys.* **2009**, *31*, 994–1001. [\[CrossRef\]](#)
24. Suzuki, K.; Aoki, K.; Ohya, K. Effects of Surface Roughness of Titanium Implants on Bone Remodeling Activity of Femur in Rabbits. *Bone* **1997**, *21*, 507–514. [\[CrossRef\]](#)
25. Wang, H.; Su, K.; Su, L.; Liang, P.; Ji, P.; Wang, C. The Effect of 3D-Printed Ti₆Al₄V Scaffolds with Various Macropore Structures on Osteointegration and Osteogenesis: A Biomechanical Evaluation. *J. Mech. Behav. Biomed. Mater.* **2018**, *88*, 488–496. [\[CrossRef\]](#) [\[PubMed\]](#)
26. Helou, M.; Kara, S. Design, Analysis and Manufacturing of Lattice Structures: An Overview. *Int. J. Comput. Integr. Manuf.* **2018**, *31*, 243–261. [\[CrossRef\]](#)

27. Gibson, L.J. Modelling the Mechanical Behavior of Cellular Materials. *Mater. Sci. Eng. A* **1989**, *110*, 1–36. [\[CrossRef\]](#)
28. Alabort, E.; Barba, D.; Reed, R.C. Design of Metallic Bone by Additive Manufacturing. *Scr. Mater.* **2019**, *164*, 110–114. [\[CrossRef\]](#)
29. Fan, H.L.; Meng, F.H.; Yang, W. Sandwich Panels with Kagome Lattice Cores Reinforced by Carbon Fibers. *Compos. Struct.* **2007**, *81*, 533–539. [\[CrossRef\]](#)
30. Xiao, Z.; Yang, Y.; Xiao, R.; Bai, Y.; Song, C.; Wang, D. Evaluation of Topology-Optimized Lattice Structures Manufactured via Selective Laser Melting. *Mater. Des.* **2018**, *143*, 27–37. [\[CrossRef\]](#)
31. Xu, S.; Shen, J.; Zhou, S.; Huang, X.; Xie, Y.M. Design of Lattice Structures with Controlled Anisotropy. *Mater. Des.* **2016**, *93*, 443–447. [\[CrossRef\]](#)
32. Yan, C.; Hao, L.; Hussein, A.; Young, P.; Raymont, D. Advanced Lightweight 316L Stainless Steel Cellular Lattice Structures Fabricated via Selective Laser Melting. *Mater. Des.* **2014**, *55*, 533–541. [\[CrossRef\]](#)
33. Zadpoor, A.A. Bone Tissue Regeneration: The Role of Scaffold Geometry. *Biomater. Sci.* **2015**, *3*, 231–245. [\[CrossRef\]](#)
34. Zhu, F.; Lu, G.; Ruan, D.; Wang, Z. Plastic Deformation, Failure and Energy Absorption of Sandwich Structures with Metallic Cellular Cores. *Int. J. Prot. Struct.* **2010**, *1*, 507–541. [\[CrossRef\]](#)
35. Maskery, I.; Aboulkhair, N.T.; Aremu, A.O.; Tuck, C.J.; Ashcroft, I.A. Compressive Failure Modes and Energy Absorption in Additively Manufactured Double Gyroid Lattices. *Addit. Manuf.* **2017**, *16*, 24–29. [\[CrossRef\]](#)
36. Burton, H.E.; Eisenstein, N.M.; Lawless, B.M.; Jamshidi, P.; Segarra, M.A.; Addison, O.; Shepherd, D.E.T.; Attallah, M.M.; Grover, L.M.; Cox, S.C. The Design of Additively Manufactured Lattices to Increase the Functionality of Medical Implants. *Mater. Sci. Eng. C* **2019**, *94*, 901–908. [\[CrossRef\]](#)
37. Strano, G.; Hao, L.; Everson, R.M.; Evans, K.E. A New Approach to the Design and Optimisation of Support Structures in Additive Manufacturing. *Int. J. Adv. Manuf. Technol.* **2013**, *66*, 1247–1254. [\[CrossRef\]](#)
38. Yan, C.; Hao, L.; Hussein, A.; Young, P.; Huang, J.; Zhu, W. Microstructure and Mechanical Properties of Aluminium Alloy Cellular Lattice Structures Manufactured by Direct Metal Laser Sintering. *Mater. Sci. Eng. A* **2015**, *628*, 238–246. [\[CrossRef\]](#)
39. Cansizoglu, O.; Harrysson, O.; Cormier, D.; West, H.; Mahale, T. Properties of Ti–6Al–4V Non-Stochastic Lattice Structures Fabricated via Electron Beam Melting. *Mater. Sci. Eng. A* **2008**, *492*, 468–474. [\[CrossRef\]](#)
40. Saini, M.; Singh, Y.; Arora, P.; Arora, V.; Jain, K. Implant Biomaterials: A Comprehensive Review. *World J. Clin. Cases* **2015**, *3*, 52–57. [\[CrossRef\]](#)
41. Aguiar, M.F.; Marques, A.P.; Carvalho, A.C.P.; Cavalcanti, M.G.P. Accuracy of Magnetic Resonance Imaging Compared with Computed Tomography for Implant Planning. *Clin. Oral Implants Res.* **2008**, *19*, 362–365. [\[CrossRef\]](#)
42. Gautam, G.; Kumar, S.; Kumar, K. Processing of Biomaterials for Bone Tissue Engineering: State of the Art. *Mater. Today Proc.* **2022**, *50*, 2206–2217. [\[CrossRef\]](#)
43. Hench, L.L.; Polak, J.M. Third-Generation Biomedical Materials. *Science* **2002**, *295*, 1014–1017. [\[CrossRef\]](#)
44. Salinas, A.J.; Esbrit, P.; Vallet-Regí, M. A Tissue Engineering Approach Based on the Use of Bioceramics for Bone Repair. *Biomater. Sci.* **2013**, *1*, 40–51. [\[CrossRef\]](#)
45. Todros, S.; Todesco, M.; Bagno, A. Biomaterials and Their Biomedical Applications: From Replacement to Regeneration. *Processes* **2021**, *9*, 1949. [\[CrossRef\]](#)
46. Guo, J.; Tan, J.; Peng, L.; Song, Q.; Kong, H.; Wang, P.; Shen, H. Comparison of Tri-Lock Bone Preservation Stem and the Conventional Standard Corail Stem in Primary Total Hip Arthroplasty. *Orthop. Surg.* **2021**, *13*, 749–757. [\[CrossRef\]](#) [\[PubMed\]](#)
47. Lenich, A.; Vester, H.; Nerlich, M.; Mayr, E.; Stöckle, U.; Füchtmeier, B. Clinical Comparison of the Second and Third Generation of IntraMedullary Devices for Trochanteric Fractures of the Hip–Blade vs. Screw. *Injury* **2010**, *41*, 1292–1296. [\[CrossRef\]](#) [\[PubMed\]](#)
48. Murphy, W.; Black, J.; Hastings, G. *Handbook of Biomaterial Properties*, 2nd ed.; Springer: New York, NY, USA, 2016. [\[CrossRef\]](#)
49. Manam, N.S.; Harun, W.S.W.; Shri, D.N.A.; Ghani, S.A.C.; Kurniawan, T.; Ismail, M.H.; Ibrahim, M.H.I. Study of Corrosion in Biocompatible Metals for Implants: A Review. *J. Alloys Compd.* **2017**, *701*, 698–715. [\[CrossRef\]](#)
50. Amiryaghoubi, N.; Fathi, M.; Pesyan, N.N.; Samiei, M.; Barar, J.; Omid, Y. Bioactive Polymeric Scaffolds for Osteogenic Repair and Bone Regenerative Medicine. *Med. Res. Rev.* **2020**, *40*, 1833–1870. [\[CrossRef\]](#)
51. Koju, N.; Niraula, S.; Fotovvati, B. Additively Manufactured Porous Ti6Al4V for Bone Implants: A Review. *Metals* **2022**, *12*, 687. [\[CrossRef\]](#)
52. Scheinpflug, J.; Pfeiffenberger, M.; Damerau, A.; Schwarz, F.; Textor, M.; Lang, A.; Schulze, F. Journey into Bone Models: A Review. *Genes* **2018**, *9*, 247. [\[CrossRef\]](#)
53. Rho, J.Y.; Kuhn-Spearing, L.; Zioupos, P. Mechanical Properties and the Hierarchical Structure of Bone. *Med. Eng. Phys.* **1998**, *20*, 92–102. [\[CrossRef\]](#)
54. Rho, J.Y.; Ashman, R.B.; Turner, C.H. Young's Modulus of Trabecular and Cortical Bone Material: Ultrasonic and Microtensile Measurements. *J. Biomech.* **1993**, *26*, 111–119. [\[CrossRef\]](#)
55. Bandyopadhyay, A.; Espana, F.; Balla, V.K.; Bose, S.; Ohgami, Y.; Davies, N.M. Influence of Porosity on Mechanical Properties and In Vivo Response of Ti6Al4V Implants. *Acta Biomater.* **2010**, *6*, 1640–1648. [\[CrossRef\]](#)
56. Buford, A.; Goswami, T. Review of Wear Mechanisms in Hip Implants: Paper I—General. *Mater. Des.* **2004**, *25*, 385–393. [\[CrossRef\]](#)
57. Kutzner, K.P.; Freitag, T.; Donner, S.; Kovacevic, M.P.; Bieger, R. Outcome of Extensive Varus and Valgus Stem Alignment in Short-Stem THA: Clinical and Radiological Analysis Using EBRA-FCA. *Arch. Orthop. Trauma Surg.* **2017**, *137*, 431–439. [\[CrossRef\]](#)

58. Bittredge, O.; Hassanin, H.; El-Sayed, M.A.; Eldessouky, H.M.; Alsaleh, N.A.; Alrasheedi, N.H.; Essa, K.; Ahmadein, M. Fabrication and Optimisation of Ti-6Al-4V Lattice-Structured Total Shoulder Implants Using Laser Additive Manufacturing. *Materials* **2022**, *15*, 3095. [[CrossRef](#)] [[PubMed](#)]
59. Arabnejad, S.; Johnston, B.; Tanzer, M.; Pasini, D. Fully Porous 3D Printed Titanium Femoral Stem to Reduce Stress-Shielding Following Total Hip Arthroplasty. *J. Orthop. Res.* **2017**, *35*, 1774–1783. [[CrossRef](#)] [[PubMed](#)]
60. Sumner, D.R. Long-Term Implant Fixation and Stress-Shielding in Total Hip Replacement. *J. Biomech.* **2015**, *48*, 797–800. [[CrossRef](#)]
61. Liverani, E.; Rogati, G.; Pagani, S.; Brogini, S.; Fortunato, A.; Caravaggi, P. Mechanical Interaction between Additive-Manufactured Metal Lattice Structures and Bone in Compression: Implications for Stress Shielding of Orthopaedic Implants. *J. Mech. Behav. Biomed. Mater.* **2021**, *121*, 104608. [[CrossRef](#)]
62. Wu, N.; Li, S.; Zhang, B.; Wang, C.; Chen, B.; Han, Q.; Wang, J. The Advances of Topology Optimization Techniques in Orthopedic Implants: A Review. *Med. Biol. Eng. Comput.* **2021**, *59*, 1673–1689. [[CrossRef](#)]
63. Kladovasilakis, N.; Tsongas, K.; Tzetzis, D. Finite Element Analysis of Orthopedic Hip Implant with Functionally Graded Bioinspired Lattice Structures. *Biomimetics* **2020**, *5*, 44. [[CrossRef](#)] [[PubMed](#)]
64. Chatzigeorgiou, C.; Piotrowski, B.; Chemisky, Y.; Laheurte, P.; Meraghni, F. Numerical Investigation of the Effective Mechanical Properties and Local Stress Distributions of TPMS-Based and Strut-Based Lattices for Biomedical Applications. *J. Mech. Behav. Biomed. Mater.* **2022**, *126*, 105025. [[CrossRef](#)]
65. Kim, T.; See, C.W.; Li, X.; Zhu, D. Orthopedic Implants and Devices for Bone Fractures and Defects: Past, Present and Perspective. *Eng. Regen.* **2020**, *1*, 6–18. [[CrossRef](#)]
66. Schaedler, T.A.; Carter, W.B. Architected Cellular Materials. *Annu. Rev. Mater. Res.* **2016**, *46*, 187–210. [[CrossRef](#)]
67. Gibson, L.J.; Ashby, M.F. *Cellular Solids: Structure and Properties*, 2nd ed.; Cambridge University Press: Cambridge, UK, 1997. [[CrossRef](#)]
68. Kladovasilakis, N.; Tsongas, K.; Kostavelis, I.; Tzovaras, D.; Tzetzis, D. Effective Mechanical Properties of Additive Manufactured Strut-Lattice Structures: Experimental and Finite Element Study. *Adv. Eng. Mater.* **2021**, *24*, 2100879. [[CrossRef](#)]
69. Kladovasilakis, N.; Tsongas, K.; Kostavelis, I.; Tzovaras, D.; Tzetzis, D. Effective Mechanical Properties of Additive Manufactured Triply Periodic Minimal Surfaces: Experimental and Finite Element Study. *Int. J. Adv. Manuf. Technol.* **2022**, *121*, 7169–7189. [[CrossRef](#)]
70. Pei, E.; Kabir, I.; Breški, T.; Godec, D.; Nordin, A. A Review of Geometric Dimensioning and Tolerancing (GD & T) of Additive Manufacturing and Powder Bed Fusion Lattices. *Prog. Addit. Manuf.* **2022**, *7*, 1297–1305. [[CrossRef](#)]
71. Kladovasilakis, N.; Tsongas, K.; Karalekas, D.; Tzetzis, D. Architected Materials for Additive Manufacturing: A Comprehensive Review. *Materials* **2022**, *15*, 5919. [[CrossRef](#)]
72. Kladovasilakis, N.; Charalampous, P.; Tsongas, K.; Kostavelis, I.; Tzetzis, D.; Tzovaras, D. Experimental and Computational Investigation of Lattice Sandwich Structures Constructed by Additive Manufacturing Technologies. *J. Manuf. Mater. Process.* **2021**, *5*, 95. [[CrossRef](#)]
73. Al-Ketan, O.; Rowshan, R.; Abu Al-Rub, R.K. Topology-Mechanical Property Relationship of 3D Printed Strut, Skeletal, and Sheet Based Periodic Metallic Cellular Materials. *Addit. Manuf.* **2018**, *19*, 167–183. [[CrossRef](#)]
74. Al-Ketan, O.; Rezgui, R.; Rowshan, R.; Du, H.; Fang, N.X.; Abu Al-Rub, R.K. Microarchitected Stretching-Dominated Mechanical Metamaterials with Minimal Surface Topologies. *Adv. Eng. Mater.* **2018**, *20*, 1800029. [[CrossRef](#)]
75. Deshpande, V.S.; Ashby, M.F.; Fleck, N.A. Foam Topology: Bending versus Stretching Dominated Architectures. *Acta Mater.* **2001**, *49*, 1035–1040. [[CrossRef](#)]
76. Ashby, M.F. The Properties of Foams and Lattices. *Philos. Trans. R. Soc. A Math. Phys. Eng. Sci.* **2006**, *364*, 15–30. [[CrossRef](#)]
77. Maskery, I.; Sturm, L.; Aremu, A.O.; Panesar, A.; Williams, C.B.; Tuck, C.J.; Wildman, R.D.; Ashcroft, I.A.; Hague, R.J.M. Insights into the Mechanical Properties of Several Triply Periodic Minimal Surface Lattice Structures Made by Polymer Additive Manufacturing. *Polymer* **2018**, *152*, 62–71. [[CrossRef](#)]
78. Parthasarathy, J.; Starly, B.; Raman, S.; Christensen, A. Mechanical Evaluation of Porous Titanium (Ti6Al4V) Structures with Electron Beam Melting (EBM). *J. Mech. Behav. Biomed. Mater.* **2010**, *3*, 249–259. [[CrossRef](#)] [[PubMed](#)]
79. Fini, M.; Giavaresi, G.; Torricelli, P.; Borsari, V.; Giardino, R.; Nicolini, A.; Carpi, A. Osteoporosis and Biomaterial Osteointegration. *Biomed. Pharmacother.* **2004**, *58*, 487–493. [[CrossRef](#)] [[PubMed](#)]
80. Agarwal, R.; García, A.J. Biomaterial Strategies for Engineering Implants for Enhanced Osseointegration and Bone Repair. *Adv. Drug Deliv. Rev.* **2015**, *94*, 53–62. [[CrossRef](#)]
81. Bobyn, J.D.; Pilliar, R.M.; Cameron, H.U.; Weatherly, G.C. The Optimum Pore Size for the Fixation of Porous-Surfaced Metal Implants by the Ingrowth of Bone. *Clin. Orthop. Relat. Res.* **1980**, *150*, 263–270. [[CrossRef](#)]
82. Bobyn, J.D.; Stackpool, G.J.; Hacking, S.A.; Tanzer, M.; Krygier, J.J. Characteristics of Bone Ingrowth and Interface Mechanics of a New Porous Tantalum Biomaterial. *J. Bone Jt. Surg. Br.* **1999**, *81*, 907–914. [[CrossRef](#)]
83. Jones, A.C.; Arns, C.H.; Huttmacher, D.W.; Milthorpe, B.K.; Sheppard, A.P.; Knackstedt, M.A. The Correlation of Pore Morphology, Interconnectivity and Physical Properties of 3D Ceramic Scaffolds with Bone Ingrowth. *Biomaterials* **2009**, *30*, 1440–1451. [[CrossRef](#)]
84. Arabnejad, S.; Burnett Johnston, R.; Pura, J.A.; Singh, B.; Tanzer, M.; Pasini, D. High-Strength Porous Biomaterials for Bone Replacement: A Strategy to Assess the Interplay between Cell Morphology, Mechanical Properties, Bone Ingrowth and Manufacturing Constraints. *Acta Biomater.* **2016**, *30*, 345–356. [[CrossRef](#)] [[PubMed](#)]

85. Bragdon, C.R.; Jasty, M.; Greene, M.; Rubash, H.E.; Harris, W.H. Biologic Fixation of Total Hip Implants. Insights Gained from a Series of Canine Studies. *J. Bone Jt. Surg. Am.* **2004**, *86* (Suppl. S2), 105–117. [\[CrossRef\]](#)
86. Harrysson, O.L.A.; Cansizoglu, O.; Marcellin-Little, D.J.; Cormier, D.R.; West, H.A. Direct Metal Fabrication of Titanium Implants with Tailored Materials and Mechanical Properties Using Electron Beam Melting Technology. *Mater. Sci. Eng. C* **2008**, *28*, 366–373. [\[CrossRef\]](#)
87. Karageorgiou, V.; Kaplan, D. Porosity of 3D Biomaterial Scaffolds and Osteogenesis. *Biomaterials* **2005**, *26*, 5474–5491. [\[CrossRef\]](#)
88. De Wild, M.; Schumacher, R.; Mayer, K.; Schkommodau, E.; Thoma, D.; Bredell, M.; Kruse Gujer, A.; Grätz, K.W.; Weber, F.E. Bone Regeneration by the Osteoconductivity of Porous Titanium Implants Manufactured by Selective Laser Melting: A Histological and Micro Computed Tomography Study in the Rabbit. *Tissue Eng. Part A* **2013**, *19*, 2645–2654. [\[CrossRef\]](#)
89. Whang, K.; Healy, K.E.; Elenz, D.R.; Nam, E.K.; Tsai, D.C.; Thomas, C.H.; Nuber, G.W.; Glorieux, F.H.; Travers, R.; Sprague, S.M. Engineering Bone Regeneration with Bioabsorbable Scaffolds with Novel Microarchitecture. *Tissue Eng.* **1999**, *5*, 35–51. [\[CrossRef\]](#)
90. Taniguchi, N.; Fujibayashi, S.; Takemoto, M.; Sasaki, K.; Otsuki, B.; Nakamura, T.; Matsushita, T.; Kokubo, T.; Matsuda, S. Effect of Pore Size on Bone Ingrowth into Porous Titanium Implants Fabricated by Additive Manufacturing: An In Vivo Experiment. *Mater. Sci. Eng. C* **2016**, *59*, 690–701. [\[CrossRef\]](#) [\[PubMed\]](#)
91. Deing, A.; Luthringer, B.; Laipple, D.; Ebel, T.; Willumeit, R. A Porous TiAl6V4 Implant Material for Medical Application. *Int. J. Biomater.* **2014**, *2014*, 904230. [\[CrossRef\]](#) [\[PubMed\]](#)
92. Levine, B.R.; Sporer, S.; Poggie, R.A.; Della Valle, C.J.; Jacobs, J.J. Experimental and Clinical Performance of Porous Tantalum in Orthopedic Surgery. *Biomaterials* **2006**, *27*, 4671–4681. [\[CrossRef\]](#) [\[PubMed\]](#)
93. Wang, C.; Xu, D.; Li, S.; Yi, C.; Zhang, X.; He, Y.; Yu, D. Effect of Pore Size on the Physicochemical Properties and Osteogenesis of Ti6Al4V Porous Scaffolds with Bionic Structure. *ACS Omega* **2020**, *5*, 28684–28692. [\[CrossRef\]](#)
94. Mullen, L.; Stamp, R.C.; Brooks, W.K.; Jones, E.; Sutcliffe, C.J. Selective Laser Melting: A Regular Unit Cell Approach for the Manufacture of Porous, Titanium, Bone in-Growth Constructs, Suitable for Orthopedic Applications. *J. Biomed. Mater. Res. Part B Appl. Biomater.* **2009**, *89B*, 325–334. [\[CrossRef\]](#)
95. Zaharin, H.A.; Abdul Rani, A.M.; Azam, F.I.; Ginta, T.L.; Sallih, N.; Ahmad, A.; Yunus, N.A.; Zulkifli, T.Z. Effect of Unit Cell Type and Pore Size on Porosity and Mechanical Behavior of Additively Manufactured Ti₆Al₄V Scaffolds. *Materials* **2018**, *11*, 2402. [\[CrossRef\]](#)
96. Yan, C.; Hao, L.; Hussein, A.; Young, P. Ti–6Al–4V Triply Periodic Minimal Surface Structures for Bone Implants Fabricated via Selective Laser Melting. *J. Mech. Behav. Biomed. Mater.* **2015**, *51*, 61–73. [\[CrossRef\]](#)
97. Ran, Q.; Yang, W.; Hu, Y.; Shen, X.; Yu, Y.; Xiang, Y.; Cai, K. Osteogenesis of 3D Printed Porous Ti6Al4V Implants with Different Pore Sizes. *J. Mech. Behav. Biomed. Mater.* **2018**, *84*, 1–11. [\[CrossRef\]](#) [\[PubMed\]](#)
98. Zheng, Y.; Han, Q.; Wang, J.; Li, D.; Song, Z.; Yu, J. Promotion of Osseointegration between Implant and Bone Interface by Titanium Alloy Porous Scaffolds Prepared by 3D Printing. *ACS Biomater. Sci. Eng.* **2020**, *6*, 5181–5190. [\[CrossRef\]](#)
99. Nouri, A.; Hodgson, P.D.; Wen, C. *Biomimetic Porous Titanium Scaffolds for Orthopedic and Dental Applications*; Mukherjee, A., Ed.; IntechOpen: Rijeka, Croatia, 2010; p. 21. [\[CrossRef\]](#)
100. Yadroitsev, I.; Shishkovsky, I.; Bertrand, P.; Smurov, I. Manufacturing of Fine-Structured 3D Porous Filter Elements by Selective Laser Melting. *Appl. Surf. Sci.* **2009**, *255*, 5523–5527. [\[CrossRef\]](#)
101. Abele, E.; Stoffregen, H.A.; Kniepkamp, M.; Lang, S.; Hampe, M. Selective Laser Melting for Manufacturing of Thin-Walled Porous Elements. *J. Mater. Process. Technol.* **2015**, *215*, 114–122. [\[CrossRef\]](#)
102. Yan, C.; Hao, L.; Hussein, A.; Raymond, D. Evaluations of Cellular Lattice Structures Manufactured Using Selective Laser Melting. *Int. J. Mach. Tools Manuf.* **2012**, *62*, 32–38. [\[CrossRef\]](#)
103. Chen, Z.; Xie, Y.M.; Wu, X.; Wang, Z.; Li, Q.; Zhou, S. On Hybrid Cellular Materials Based on Triply Periodic Minimal Surfaces with Extreme Mechanical Properties. *Mater. Des.* **2019**, *183*, 108109. [\[CrossRef\]](#)
104. Kladovasilakis, N.; Tsongas, K.; Tzetzis, D. Development of Novel Additive Manufactured Hybrid Architected Materials and Investigation of Their Mechanical Behavior. *Mech. Mater.* **2023**, *176*, 104525. [\[CrossRef\]](#)
105. Kladovasilakis, N.; Charalampous, P.; Kostavelis, I.; Tzetzis, D.; Tzovaras, D. Impact of Metal Additive Manufacturing Parameters on the Powder Bed Fusion and Direct Energy Deposition Processes: A Comprehensive Review. *Prog. Addit. Manuf.* **2021**, *6*, 349–365. [\[CrossRef\]](#)
106. Khrapov, D.; Kozadayeva, M.; Manabaev, K.; Panin, A.; Sjöström, W.; Koptug, A.; Mishurova, T.; Evsevlev, S.; Meinel, D.; Bruno, G.; et al. Different Approaches for Manufacturing Ti-6Al-4V Alloy with Triply Periodic Minimal Surface Sheet-Based Structures by Electron Beam Melting. *Materials* **2021**, *14*, 4912. [\[CrossRef\]](#)
107. Evsevlev, S.; Mishurova, T.; Khrapov, D.; Paveleva, A.; Meinel, D.; Surmenev, R.; Surmeneva, M.; Koptug, A.; Bruno, G. X-ray Computed Tomography Procedures to Quantitatively Characterize the Morphological Features of Triply Periodic Minimal Surface Structures. *Materials* **2021**, *14*, 3002. [\[CrossRef\]](#)

Disclaimer/Publisher’s Note: The statements, opinions and data contained in all publications are solely those of the individual author(s) and contributor(s) and not of MDPI and/or the editor(s). MDPI and/or the editor(s) disclaim responsibility for any injury to people or property resulting from any ideas, methods, instructions or products referred to in the content.